Flooding Patterns of the Okavango Wetland in Botswana between 1972 and 2000

Author(s): Jenny M. McCarthy, Thomas Gumbricht, Terence McCarthy, Philip Frost, Konrad Wessels, and Frank Seidel

Source: AMBIO: A Journal of the Human Environment, 32(7):453-457. 2003.
Published By: Royal Swedish Academy of Sciences
DOI: http://dx.doi.org/10.1579/0044-7447-32.7.453
URL: http://www.bioone.org/doi/full/10.1579/0044-7447-32.7.453

Jenny M. McCarthy, Thomas Gumbricht, Terence McCarthy, Philip Frost, Konrad Wessels and Frank Seidel

Flooding Patterns of the Okavango Wetland in Botswana between 1972 and 2000

The inundated area of the Okavango Delta changes annually and interannually. The variability relates to regional precipitation over the catchment area in the Angolan highlands, and to local rainfall. The patterns of the wetland were captured using more than 3000 satellite images for the period 1972 to 2000, near daily NOAA AVHRR data for 1985-2000, and less frequent images of the Landsat sensors from 1972 onwards. One AVHRR image for every 10-day period was classified into land and water using an unsupervised classification method. Evaluation against Landsat TM and ERS2-ATSR data indicate an agreement of 89% for the size of estimated inundation area. Results show that the wetland area has varied between approximately 2450 km^2 and 11 400 km^2 during the last 30 years.

INTRODUCTION

The Okavango Delta in northern Botswana (Fig. 1) is one of the world's largest inland deltas and is situated on an alluvial fan nearly 40 000 km^2 in size. The Delta consists of swamps, islands and river channels in a shifting mosaic. The wetland is fed by local summer rains (~6 x 10^9m^3 yr^{-1}), and is flooded annually when the floodwaters from the Angolan highlands arrive with the Okavango River between February and May (~9 x 10^9 m^3 yr^{-1})(1). The flood reaches the lower parts of the Delta 3 to 4 months after the peak in the Delta entry channel – the Panhandle (Fig. 1). The period of maximum inundation is normally in winter (May – September), gradually decreasing to a low in summer (November – March). The wetland can hence be divided into a permanent and a seasonal swamp. Only a small fraction of the flow is discharged from the wetland to the Boteti River, as about 97% of the incoming water is lost by evapotranspiration (2).

The catchment of the Okavango River is shared by Angola, Namibia and Botswana, and in periods of drought the freshwater of the river and wetland becomes a valuable potential water source in the dry Kalahari environment. Fears of a possible future conflict over the water have fuelled research with the goal of describing and predicting water flow. However, hydrological models have only been developed for predicting the outflow in the Boteti River, and have not focused on seasonal flooding and spatial patterns, which are ecologically far more important (2). Estimates of historical flooding are a prerequisite for predictive modelling of the hydrological effects of both natural and man-made changes in the catchment and climate. The aim of this study has been to quantify flooded area and flooding patterns over the last 30 years using available remotely sensed data. The use of satellite images is essential as the wetland is largely inaccessible on the ground.

The annual variation in water recharge to the Okavango Delta is high, and the extent of flooding and the spatial advancement of the flood wave are poorly understood. Inter-annual variations have also been observed, with a general decline of recharge since 1980 (3). Over the past 2 centuries historical records reveal that the channel distribution on the Delta has changed (4, 5) and that the flooded area has shifted. These changes are believed to be induced by external climate changes and El Niño/Southern Oscillation (ENSO) effects, and by internal factors including sedimentation, channel blockage and avulsion (4).

The quoted size of the Okavango wetland differs between sources, ranging from 3000 to 16 000 km^2 (6-12). Examples of the use of satellite images for inundation area analysis exist for Okavango, but only for limited time periods or in global data sets (2, 11, 12). Multitemporal studies describing the spatial changes in the flooding over a longer period of time, utilizing the full range of available satellite data, have not previously been conducted.

In this study, more than 3000 satellite images, mainly from the NOAA AVHRR sensors, supplemented with Landsat data, were employed to gain knowledge of the recent flooding patterns in Okavango, showing the seasonal and inter-annual changes in wetland size and distribution for the period 1972 to 2000.

Figure 1. The Okavango Delta in Botswana, with selected digitized rivers projected on a Landsat TM mosaic image. The coordinates are given in kilometers.

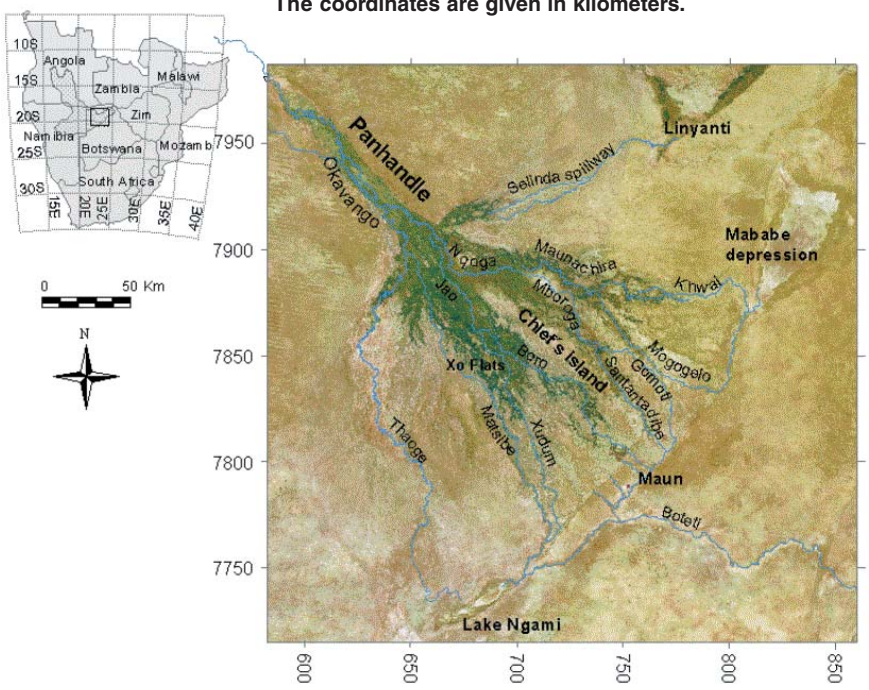

MATERIAL AND METHODS

Satellite Data

NOAA Advanced Very High Resolution Radiometer (AVHRR) satellite images were the main data source for estimating inundation. Nearly 3000 images were available for the period 1985 to 2000 (Table 1). Standard geometric corrections were applied using both orbital and Ground Control Point (GCP) information. Radiometric corrections on the visible and near-infrared channels were made using the post-launch calibration formulae presented by Rao and Chen (13), derived by calculation of top-of-the-atmosphere albedo for a 10-year period at stable calibration sites. The method is based on the regression relationship between the slope of the albedo for each channel and the elapsed time in orbit, expressed in days after launch. A subset of images (one image per 10-day period, in total 381 out of 2951 images) was selected from an automated cloud detection algorithm. Clouds were masked out in the AVHRR data using thresholds in channels 2 (0.9 μm) and 4 (11 μm) and a distance function from the identified clouds was applied to decrease cloud shadow contamination. Hence, pixels falling within 2.5 km from an identified cloud were eliminated. Images near the center of the swath width were ideally selected to minimize geometric observation effects; however, in the rainy summer months the occurrence of clouds determined the image selection. The selected scenes were manually georeferenced in east-west, north-south directions. The data were projected to Universal Transverse Mercator (UTM) S 34, using the Cape datum (Central meridian: 21; Scale factor: 0.9996; False Easting: 500 000; False Northing: 10 000 000) in 1-km resolution. Landsat Multispectral Scanner (MSS) and Thematic Mapper (TM) data in 500 m resolution, projected to the same coordinate system, were used for dates earlier than 1985. ERS-2 Along Track Scanning Radiometer (ATSR) and Landsat TM and Enhanced TM (ETM) scenes were used for calibration and evaluation of classification accuracy.

Table 1. Satellite data used in the inundation study.

Sensor	No. of scenes	Acquisition years / periods/ dates
NOAA AVHRR (9, 11, 14)	381 (selected from 2951)	1985 – 1988, 1990 – 2000
ERS-2 ATSR	28	Aug. – Dec. 1999, Mar. – Nov. 2000
Landsat MSS	44	1972, 1979, 1984, 1985
Landsat TM	34	1984, 1985, 1987, 1988, 1994, 1995
Landsat ETM	18	1999, 2000

Water Identification

Deep waterbodies with a free surface are comparatively easy to detect in satellite data, whereas shallow wetlands covered with vegetation are more difficult to classify as the signal then includes constituents other than water. Various methods are commonly used for classifying wetlands, such as thresholding and ratioing between channels, or supervised and unsupervised classifications (14). Supervised classification uses area statistics based on sample training to classify an image, whereas unsupervised classifications involve algorithms that examine a large number of unknown pixels and divide them into a number of classes based on natural groupings (15). In this study, an automated routine for supervised maximum likelihood classification was initially tested, using a set of training areas representing known permanently flooded and dry areas in the images. Initial cloud detection determined which training areas to use for each scene. Due to geometric inaccuracies, radiometric problems related to the use of different sensors, and remains of cloud shadows and other atmospheric disturbances, the supervised classification method had to be rejected. A ratioing and thresholding formula including all channels (NOAA AVHRR) was also tested for the classification, but due to the radiometric problems all images needed manual calibration of the formula. In the end, unsupervised classification in 15-30 classes was used for distinguishing between land and water (Fig. 2). The 381 AVHRR scenes selected from the cloud algorithm were classified, using all channels. Extending back in time, Landsat data prior to 1985 and for the year 1986 were used for estimating flooding independently for 8 months (November 1972, May-June 1979, May-August 1984, November 1986). The Okavango Delta covers 4 Landsat scenes, and for each of these dates at least 3 Landsat scenes were available. If needed, the data gap (i.e. the 4th quadrant) was filled by dates with similar flooding patterns to the other 3.

Calibration of the thresholds specifying the water classes from the unsupervised classification, and of weighting of filtering, was set by using Landsat and ATSR scenes for comparison. 10 Landsat MSS/TM images spanning February to September (1985-1988) were used, and 12 ATSR images spanning March to November (2000). For ATSR data, water was extracted using unsupervised classification, while the water classification of the Landsat scenes was done from manually identified training areas as supervised classification. For the unsupervised classifications

Figure 2. Classification steps a) original AVHRR scene (rgb 1,2,3) (date 25 August 1998); b) unsupervised classification in 10 classes; and c) water – land classification.

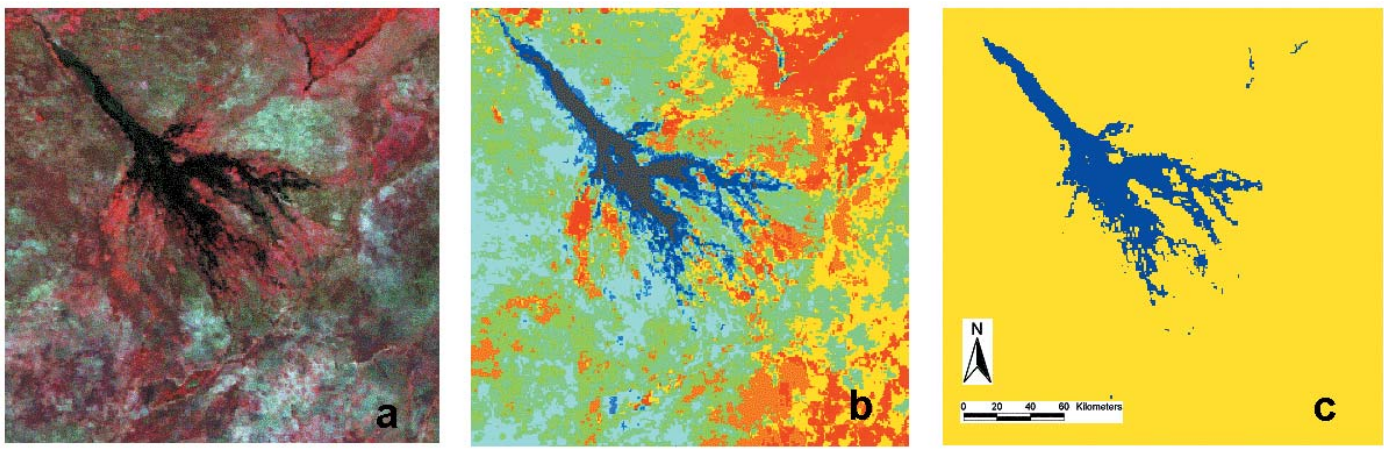

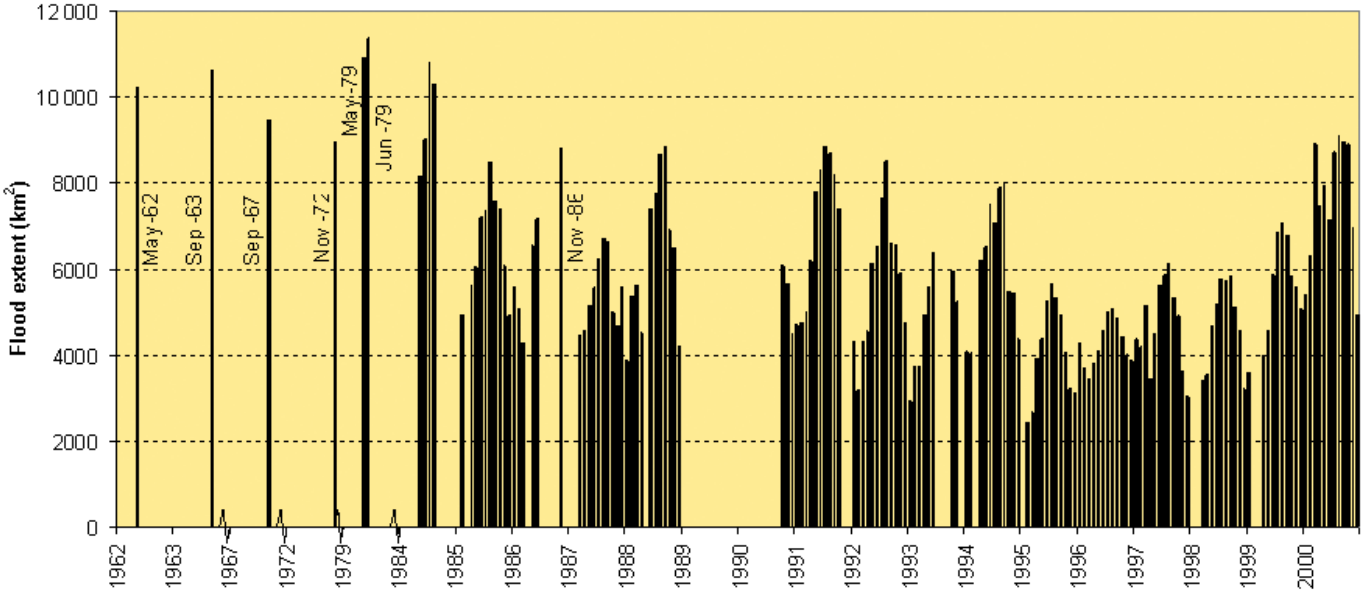

Figure 3. Monthly area of inundation for the years between 1985 and 2000 (in km²), classified from NOAA AVHRR satellite images. The zero-values indicate gaps in the data series. Note the breaks in the x-axis before 1984.

the water area was always maximized until pixels also outside the Okavango wetland entered the inundation class – this last class was then omitted. Most of the calibration scenes cover only part of the Okavango. Hence, the calibration only used visual inspection of the coherence between the AVHRR classification and the reference (ATSR/Landsat) classification.

A 3-dimensional contextual and weighted filter, using the preceding and following 10-day images as the third dimension, smoothed the water classification. Pixel locations with clouds were handled by seeking the closest cloud-free image for that pixel. A maximum limit was set at 30 days, with back and forth searching for the closest image with data. If no cloud-free image was available within +/- 1 month, the average flooding situation for that particular date (i.e. month) was used to determine flooding status. At those locations inundated more than 95% of cloud-free time, the cloudy pixels were directly translated as water. This approach could not be evaluated due to lack of reference data for the cloudy summer months.

Scattered rain puddles were present in the images from the rainy season. As the main focus was on the flood, small (< 3 km²) temporary rain pools were eliminated by comparing the scattered water pixels with filtered images from preceding and following dates. If the pools did not last longer than 1 month they were classified as land pixels. The use of filtered images was necessary to compensate for the effects of geoposition mismatch.

The classifications were evaluated against 6 Landsat and 6 ATSR scenes (Table 2) for single occasions corresponding to the AVHRR dates. The Landsat and ATSR classifications were regarded as "true" inundation data in the evaluation, a simplification made due to the high spatial resolution of Landsat and high radiometric quality of ATSR. Total and coinciding areas of inundation between the estimated floods were calculated.

Apparent problems with the classification of the anomalously large 2000 spring-flood (after heavy local rains) were solved by including 7 ATSR calibration scenes in the classification (dates 8 March 2000 –– 20 May 2000). As Landsat data were available for evaluation of the same period (Table 2) the inclusion of calibration data to the model data could be justified.

In a final step, after evaluation, the 10-day images were translated to represent monthly flooding. Each image was filtered by a mean filter with double weight for the central pixel, to further generalize the flooding pattern. Individual images and filtered versions of those images, representing a particular month, were then averaged.

Table 2. Accuracy evaluation results derived from cross tabulation of classification and reference data.

Date	AVHRR (km²)	Date	Reference Landsat (km²)	AVHRR correct (%)
5 July 1994	7387	7 Jul. / 1 Aug. 1994	7126	86%
4 Dec. 1994	(4891)	7 Dec. / 14 Dec. 1994	(4926)	78% (only part of image)
15 Feb. 1995	(2539)	16 Feb. 1995	(3785)	81% (only part of image)
7 Oct. 1999	6332	10 Oct. / 2 Nov. 1999	6326	84%
7 Apr. 2000	7936	3 Apr. / 10 Apr. 2000	7958	85%
8 Sept. 2000	8518	1 Sept. / 10 Sept. / 2 Nov. 2000	8192	87%
			Reference ATSR (km²)	
25 Aug. 1999	7226	30 Aug. 1999 (8 Sept. 1999)	6902	87%
3 Sept. 1999	7042	2 Sept. 1999 (8 Sept. 1999)	6992	89%
19 Sept. 1999	6562	18 Sept. / 21 Sept. 1999	5675	79%
28 Sept. 1999	(6532)	24 Sept. 1999	(6034)	85% (only part of image)
7 Oct. 1999	(5804)	4 Oct. 1999	(4706)	73% (only part of image)
16 Dec. 1999	(5377)	16 Dec. 1999	(4026)	63% (partly cloudy)

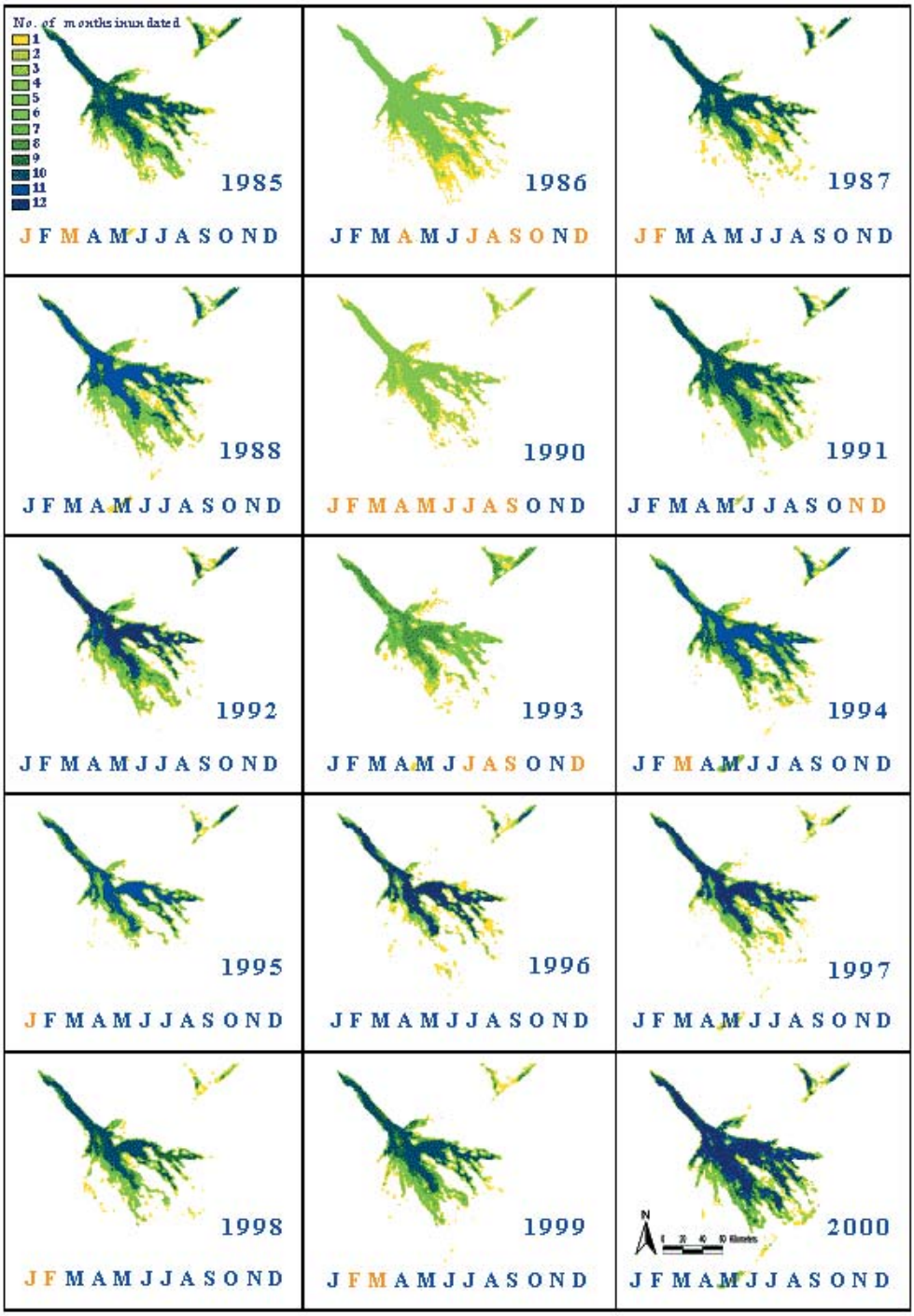

Figure 4. Yearly inundation from 1985 to 2000 (1989 lacking), classified from NOAA AVHRR satellite images. The legend categories refer to the number of months of inundation (average monthly values). The letters below the maps refer to months (January to December) where months with missing data are colored yellow.

RESULTS

The size discrepancy in total flooded area between the AVHRR estimated floods against ATSR/Landsat estimated floods (columns 2 and 4 in Table 2) varies between 6 and 1351 km^2, averaging at 509 km^2, or 11%. The spatial discrepancy is given as the percentage of the AVHRR derived flooding falling inside the ATSR/Landsat derived flood (column 5 in Table 2). This spatial accuracy varies between 63% and 89% (79% – 89% for full scenes).

The interannual flood results show that the most widespread inundation in the data series was in June 1979 and covered 11 382 km^2 (Fig. 3). The year with the smallest area of inundation was 1996 with a maximum of 5094 km^2 in August, i.e. less than half the size of the flood in 1979 (Figs 3 and 4). The maximum floods occur in July-August and the minimum floods in January-February (Fig. 3). The flooding duration for the whole period is summarized in Figure 5.

DISCUSSION

Both the seasonal and interannual variations of the inundated area in the Okavango Delta could be observed from classifications of NOAA AVHRR and Landsat satellite images. The size of the estimated inundation area agrees well with reference data, on average at 89%. The large inundation area for the year 2000 is due to local rainfall over the Delta rather than floods derived from rainfall in the Angolan highlands (Gumbricht et al., submitted). As a consequence, these floods came earlier in the season compared to previous years. The extent to which the flooding pattern for previous years was dependent on local precipitation *versus* inflow *via* the Okavango River is presently being analyzed. Here the main problem is an almost total lack of rainfall station data from Angola from 1972 to the present.

The study adds quantitative estimates to the general knowledge of the flooding pattern of the Okavango. During low flow the flooded area is confined to the middle and lower panhandle, and

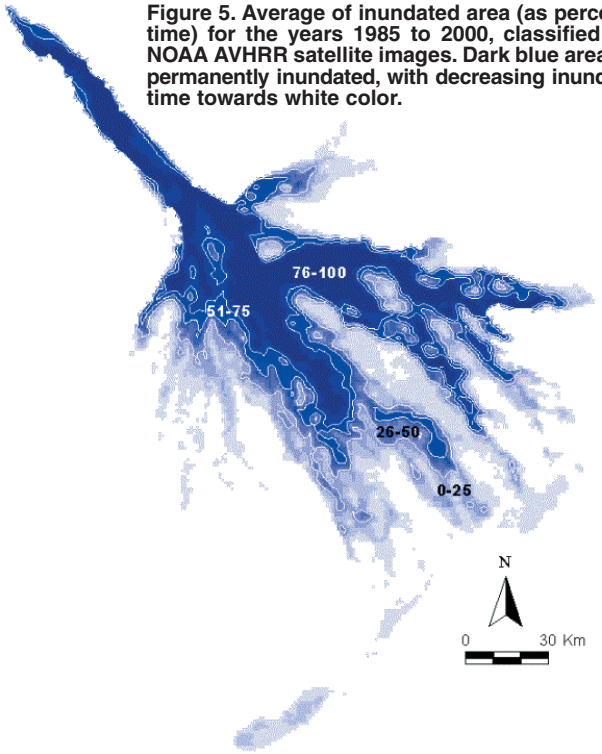

Figure 5. Average of inundated area (as percent of time) for the years 1985 to 2000, classified from NOAA AVHRR satellite images. Dark blue areas are permanently inundated, with decreasing inundation time towards white color.

to the river systems to the north and northeast of Chief's island (Nqoga-Maunachira-Mboroga-Santantadibe) (Fig. 1). The flood then expands from April onwards at the time when the Okavango River reaches peak flow in the upper panhandle and starts recharging the Delta. Notable is the flooding of the large Xo flats in the middle of the Delta, west of Chief's island. At maximum flooding in the Delta, water can be identified in the Boteti River outlet, but only a small fraction (1-2%) of the incoming water actually exits the Delta as surface discharge (9). Of the major arms of the Delta the most westerly (Thaoge) is clearly dormant, while the central arm (Jao-Boro) has the most pronounced seasonal variation, and the easterly (Nqoga-Maunachira) has a rather constant extension (Fig. 5).

In spite of the restrictions caused by the coarse (1.1 km) resolution, we believe that the size variations of the flood are well captured with the NOAA AVHRR data. The major strength of this approach is multitemporality, allowing for estimations over a longer time period.

CONCLUSIONS

Seasonal and interannual variations of the inundated area of the Okavango Delta were observed employing unsupervised classification of NOAA AVHRR, ERS-2 ATSR and supervised classification of Landsat satellite imagery. The inundation patterns of the wetland were captured using more than 3000 images for the period 1972 to 2000. This study is the first attempt to map the inundated area of Okavango utilizing such a large number of satellite images, and it adds quantitative estimates of the general knowledge of the flooding patterns. The major flooding extent is presently to the middle and eastern Delta, maximum flood is in July-September and the minimum flood occurs in January-February. The area of the wetland has varied between approximately 2450 km^2 and 11 400 km^2 during the 30 years covered by the satellite data. The minimum flood area was in February 1996, followed by 4 years of increased inundation area. The derived inundation maps are presently used for calibration and validation in distributed hydrological modelling, with the aim of providing a scientific basis for decisions concerning the water resources of the Okavango Delta.

References and Notes

1. Wilson, B.H. and Dincer, T. 1976. An introduction to the hydrology and hydrography of the Okavango Delta. In: *Symposium on the Okavango Delta*, Botswana Soc., Gaborone, Botswana, pp. 33-48.
2. McCarthy, T.S., Bloem, A. and Larkin P.A. 1998. Observations on the hydrology and geohydrology of the Okavango Delta. *S. Afr. J. Geol. 101*, 101-117.
3. McCarthy, T.S., Cooper, G.R.J., Tyson, P.D. and Ellery, W.N. 2000. Seasonal flooding in the Okavango Delta, Botswana – recent history and future prospects. *S. Afr. J. Sci. 96*, 25-33.
4. McCarthy, T.S. and Ellery, W.N. 1998. The Okavango Delta. *Trans. Roy. Soc. S. Afr. 53*, 157-182.
5. Wilson, B.H. 1973. Some natural and man made changes of the Okavango Delta. *Botswana Notes Records 5*, 132-153.
6. Ellery, K., Ellery, W.N., Rogers, K.H. and Walker, B.H. 1991. Water depth and biotic insulation: major determinants of backswamp plant community composition. *Wetlands Ecol. Mgmt 1*, 149-162.
7. McCarthy, T.S. 1993. The great inland deltas of Africa. *J. Afr. Earth Sci. 17*, 275-291.
8. Ellery, K and Ellery, W. 1997. *Plants of the Okavango Delta, A Field Guide.* South Africa: Tsaro Publishers.
9. Gieske, A. 1997. Modelling outflow from the Jao/Boro River system in the Okavango Delta, Botswana. *J. Hydrol. 193*, 214-239.
10. Ashton, P. and Manley, R. 1999. Potential hydrological implications of water abstraction from the Okavango River in Namibia. In: *Proc. Ninth South African National Hydrological Symposium, University of the Western Cape,* Bellville, 29-30 November 1999. 11 pp.
11. Gumbricht, T., McCarthy J. and McCarthy, T.S. 2000. Portraying the geophysiology of the Okavango Delta, Botswana. *Proc. 28th International Symposium on Remote Sensing of Environment,* 27-31 March 2000, Cape Town, South Africa. CD-ROM publication, ICRSE, 4: 10-13.
12. Prigent, C., Matthews, E., Aires, F. and Rossow, W.B. 2001. Remote sensing of global wetland dynamics with multiple satellite data sets. *Geophys. Res. Letters 28*, 4631-4634.
13. Rao, C.R.N. and Chen, J. 1999. Revised post-launch calibration of the visible and near-infrared channels of the Advanced High Resolution Radiomenter (AVHRR) on the NOAA014 spacecraft. *Int. J. Remote Sens. 20*, 3485-3491.
14. Birkett, C.M. 2000. Synergistic remote sensing of Lake Chad: Variability in basin inundation. *Remote Sens. Environ. 72*, 218-236.
15. Lillesand, T.M. and Kiefer, R.W. 1994. *Remote Sensing and Image Interpretation*. John Wiley and Sons Inc., New York. 750 pp.
16. This study was part of the SAFARI 2000 Southern African Regional Science Initiative, and partly financed by the Swedish International Development Cooperation Agency (Sida).
17. First submitted 29 May 2002. Revised version received 28 Nov. 2002. Accepted for publication 29 Nov. 2002.

Jenny McCarthy holds a PhD from the Royal Institute of Technology in Stockholm. She is specializing in remote sensing of land cover and various landscape features, applied in several studies of the Okavango Delta. Her address: Department of Land and Water Resources Engineering, Royal Institute of Technology, SE-100 44 Stockholm, Sweden.
jennymcc@kth.se

Thomas Gumbricht holds a PhD from the Royal Institute of Technology in Stockholm. He has been head of geoinformatics at the Department of Earth Sciences, Uppsala University, and has recently been a postdoc at the University of the Witwatersrand, working with the Okavango Delta for the past 3 years. His address: Tema Vatten, Linköping University, SE-581 83 Linköping, Sweden.
thomas_gumbricht@hotmail.com

Terence McCarthy is a professor in geochemistry and has conducted research in the Okavango Delta since the mid-1980s. His address: Department of Geology University of the Witwatersrand, Private Bag 3, 2050 Wits, South Africa.
mccarthyt@geosciences.wits.ac.za

Philip Frost is a remote sensing researcher at the Institute for Soil, Climate and Water. He is currently busy with his Master's degree looking at fire frequency in southern Africa. His address: Institute for Soil, Climate and Water, Private Bag X79, Pretoria 0001, South Africa.
pfrost@iscw.agric.za

Konrad Wessels is a PhD student at the University of Maryland. He has also been an employee of the Institute for Soil, Climate and Water during the research of the report. His address: Department of Geography, University of Maryland, 2181 LeFrak Hall, Collage Park, MD 20742, USA.
wessels@neelix.umd.edu

Frank Seidel is a student of geodesy at the Technical University of Dresden, Germany.
frank_sdl@gmx.de